1

Hydraulic Fracture Geometry from Mineback Mapping

R. G. Jeffrey

SCT Operations Pty. Ltd., Wollongong, New South Wales, Australia

KEY POINTS

- Details of full-size hydraulic fracture geometry are only available from mapping of mined fractures.
- Hydraulic fractures mapped in naturally fractured coal, sandstone, and in crystalline rock show many similarities that result from interactions with natural fractures and shear structures.

1.1 Introduction

Hydraulic fractures have been mapped during mining in a range of rock types and in a variety of geologic and in situ stress settings. Mapping has occurred for fractures placed into clay and soil [1], welded tuff [2], coal ([3–5]), andesite [6], and other crystalline and metamorphic rocks in porphyry ore bodies [7–9].

Coal seams are typically fractured for the purpose of stimulating production of seam gas (coalbed methane), either for commercial use of the gas or to improve drainage of gas from the coal before mining. Approximately 50 hydraulic fractures have been mined and mapped in detail in coal seams in the United States and Australia ([3, 4, 10, 11]; Jeffrey et al. 1993). In comparison, fractures mapped in other materials (soil and rock) total less than 20, with 10 of these located in porphyry copper and gold orebodies ([6, 7, 9]; containing intrusive monzonites and metamorphosed volcanic sediments. These fractures were placed as part of investigations into fracture geometry expected to be produced by hydraulic fractures used to precondition the orebody in advance of mining. The fractures placed into welded tuff were part of early research into hydraulic fracture growth [2] and the soil fractures were part of a study of fracturing for waste remediation [1].

By comparing the fracture geometry mapped in these different natural materials, common and disparate features of the fractures are highlighted. To help with the comparison, dimensionless groups that have been shown to be important in hydraulic fracture growth are calculated or estimated for each mapped fracture. There is an extensive body of work using experimental, analytical, and numerical methods to investigate interactions of hydraulic fractures with bedding and natural fractures and faults. This paper limits itself to the mapped geometry exposed by mining of full-size hydraulic fractures and presents a comparison of features found in coal, sandstone, and stronger metamorphic or igneous rocks.

1.2 Summary of Mapped Fracture Geometries

Selected hydraulic fractures that were placed in coal, sandstone, and hard rock are described in this section. For each fracture the treatment parameters, rock properties, and in situ properties are listed.

1.2.1 Fractures in Coal

Two fractures placed into coal seams will be described, one located in Australia as described by Jeffrey et al. (1993) and one located in the United States [10]. The fracture descriptions include details of the treatment and site characterization, including rock mechanical properties and in situ stress data.

Mechanics of Hydraulic Fracturing: Experiment, Model, and Monitoring, First Edition.
Edited by Xi Zhang, Bisheng Wu, Diansen Yang, and Andrew Bunger.

1.2.1.1 DHM-7 Fracture

As part of a program to better understand hydraulic fracture stimulation of coal, well DHM-7 was fractured using linear gel with sand proppant [10]. DHM-7 was drilled and completed open hole through the Blue Creek coal seam in Alabama. The well was located over the Oak Grove Mine in the Warrior Basin. Table 1.1 summarizes the parameters of the site and the treatment parameters. It is difficult to measure σ_H in coal because the cleat and natural fractures make overcoring impractical and the determination of fracture initiation is difficult when using a microfrac stress test. A value for σ_H that is larger than the vertical stress has been selected because the mine back mapping revealed no development of propped fractures at right angles to the direction of the main vertical fracture branch.

Room and pillar mining exposed the fracture in the coal rib around the sides of two pillars and along the coal rib nearest the well (Figure 1.1). A vertical and horizontal propped fracture (T-shaped) was found with the vertical part consisting of a number of parallel strands. The vertical fracture extended for more than 30 m to the north of the well. A horizontal propped fracture, extending over the vertical fracture, was located at the coal-roof rock interface and was mapped in detail (see Figure 1.2). The fracture was not mined to the south, but based on the area and fracture widths mapped, the propped fracture mapped on the north side of well DHM-7 was estimated to contain approximately 75% of the sand proppant injected [12].

The treatment pumped into DHM-7 used a non-crosslinked guar-based gel fluid that was injected at an average rate of 8.3 barrels/min (0.022 m^3/s). A thick resin-coated sand system was pushed into the near-well part of the fracture on the morning following the main treatment. This resin coated sand was used to test its ability to stabilize the wellbore region. It is designed to retain 80% of the sand's permeability after curing. Much of the vertical fracture exposed nearest the wellbore, at location A in Figure 1.1, was filled with this resin-coated sand. Samples of this propped fracture were excavated and taken from the mine for later analysis and display. No resin-coated sand was found at the next exposure at location B. Mapping of the horizontal fracture was done at the detail level represented in Figure 1.2 along all propped exposures.

The mapped geometry in DHM-7 and other cases presented below rely on the proppant to mark the fracture path. The hydraulic fracture typically extends beyond the proppant, especially when less viscous fluids are used. Hydraulic fractures cannot in general be found or mapped if they do not contain proppant. The distribution of the proppant, especially in a horizontal fracture, depends on both the fracture width and the fluid velocity field. Proppant transport in horizontal fractures is an area of study that has received little attention, primarily because horizontal fracture growth is thought to be a rare occurrence at depths greater than approximately 300 m. The hydraulic fractures described below that were placed into the orebody at Northparkes at a depth of 580 m were horizontal. T-shaped fractures are common in stimulation of coal and better models that can deal with horizontal fracture growth and the associated proppant transport problem would be welcome.

Table 1.1 DHM-7. Coal, well, and treatment parameters.

Parameter	Value	Units	Description
σ_H	>8.1	MPa	Maximum horizontal stress
σ_h	6.2	MPa	Minimum horizontal stress
σ_v	8.1	MPa	Vertical stress
P_o	<3	MPa	Pore pressure (estimated)
k	1.2	md	Permeability, millidarcy
E	4000	MPa	Young's modulus of coal
ν	0.3		Poisson's ratio of coal
Q	0.022	m^3/s	Injection rate
μ	25×10^{-9}	MPa s	Apparent fluid viscosity, at 170 s^{-1}
Depth	331.3	m	Depth to top of Blue Creek seam
r	0.108	m	Wellbore radius

1.2.1.2 DDH 190 Fracture

An uncased HQ-size cored borehole (DDH 190) was drilled through the German Creek coal at Central Colliery in Queensland and was hydraulically fractured using a borate crosslinked hydroxypropyl guar gel fluid. The site was characterized by undertaking well testing, stress measurement, core testing, and fracture testing before the main fracture treatment. Table 1.2 summarizes the site parameters relevant to the treatment as given by Jeffrey et al. [5].

Mapping of the fracture during and after development of the roadways in this area of the mine revealed a vertical fracture in the coal that extended into the roof rock (Figure 1.3). The fracture trace in the roof rock (Figure 1.3a) was primarily a single fracture, but interactions with natural fractures resulted in the formation of some offsets and short parallel branches. The vertical fracture trace in the coal at the north side of 13 cut-through (Figure 1.3b) was typical of other vertical sections mapped at this site, consisting of a single fracture that interacted with bedded and sheared coal. The 150 mm-thick mid-seam shear zone (mssz) runs through much of the German Creek seam and is composed of sheared coal, with particles

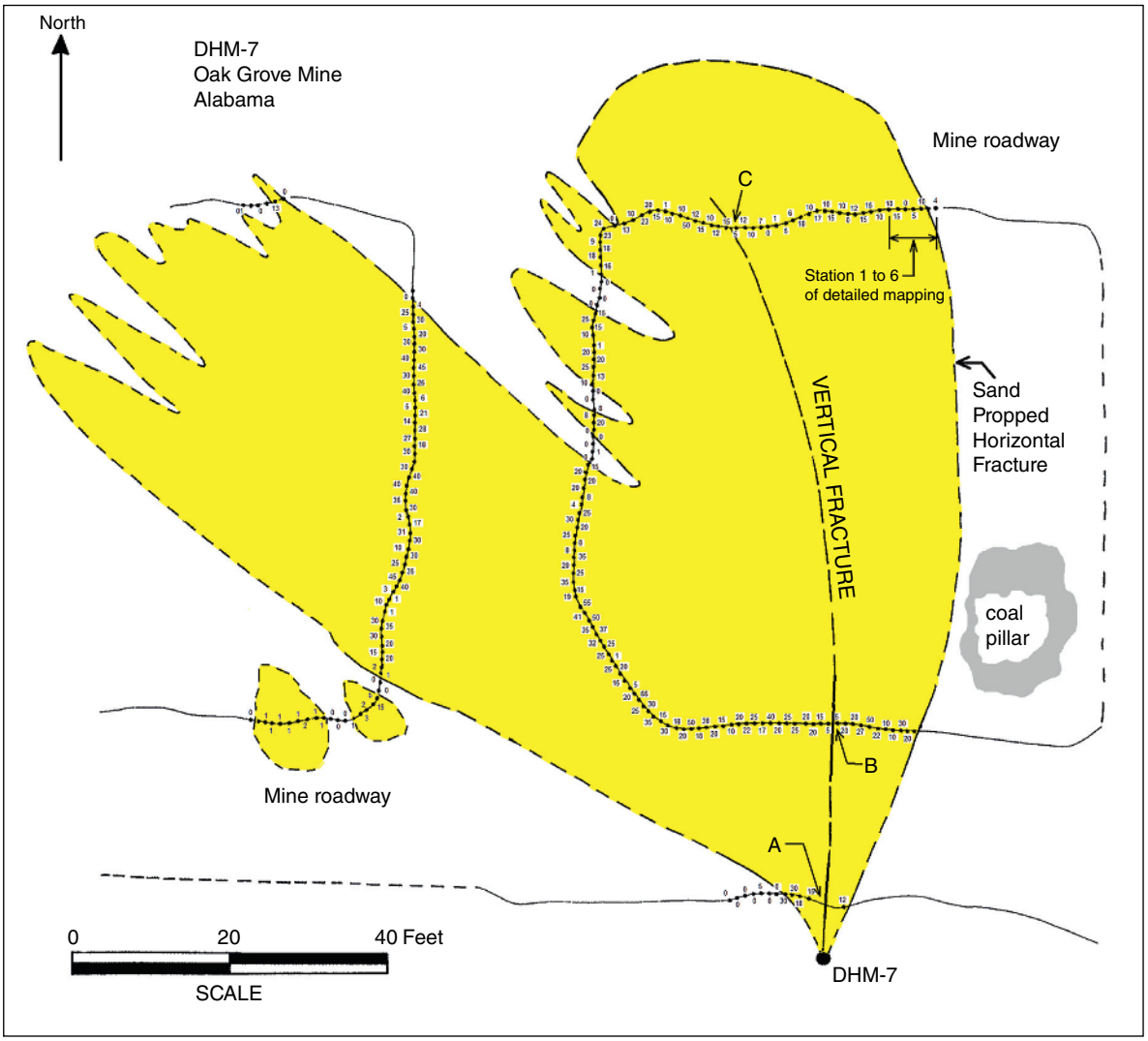

Figure 1.1 A plan view of the propped hydraulic fracture mapped at the DHM-7 site is shown in the top drawing while three mapped vertical fracture sections exposed at the coal rib are shown in the lower drawing. Mapping of the horizontal fracture occurred along the ribs of the roadways where the fracture was exposed near the roof (*Source:* Boyer et al. [12]/Gas Research Institute).

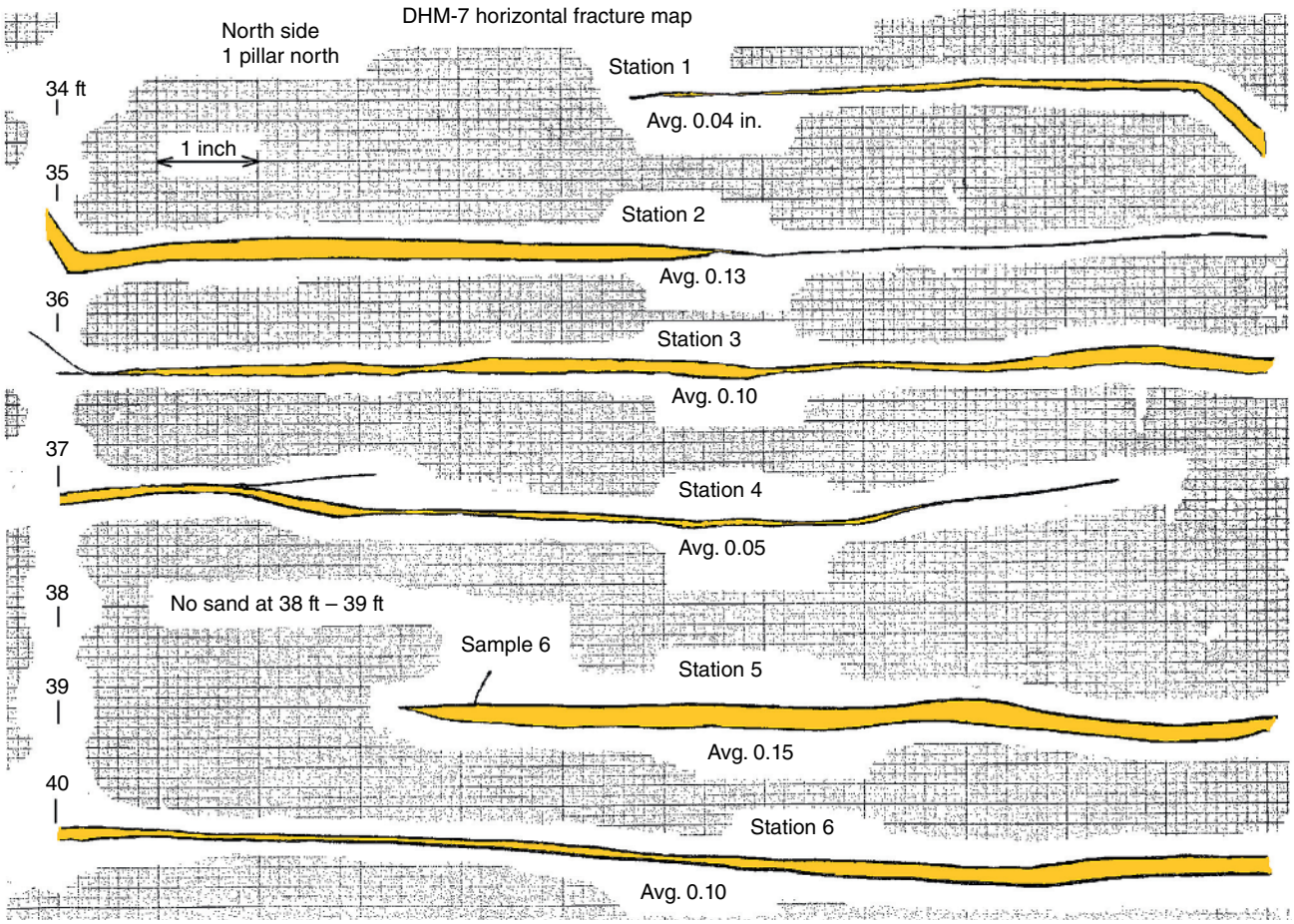

Figure 1.2 Seven linear feet of horizontal fracture mapped along the north side of the coal pillar (*Source:* Boyer et al. [12]/Gas Research Institute). The location of this portion of the horizontal fracture is indicated in Figure 1.1 and labeled as station 1 through 6. The entire horizontal fracture was mapped at this level of detail and the numbers in Figure 1.1 along the pillar boundary indicate the average propped width in hundredths of inches (e.g. 30 represents 0.30 in.).

Table 1.2 DDH 190 site parameters.

Parameter	Value	Units	Description
σ_H	>4	MPa	Max horizontal stress, in roof
σ_h	2.5	MPa	Min horizontal stress in coal
	1.9	MPa	Min horizontal stress in roof
σ_v	4.5	MPa	Vertical stress
P_o	1.08	MPa	Pore pressure
k	4.2	md	Permeability, millidarcy
E	2 000	MPa	Young's modulus, coal
	25 000	MPa	Young's modulus, roof rock
ν	0.35		Poisson's ratio, coal
	0.13		Poisson's ratio, roof rock
Q	0.002 5	m^3/s	Injection rate
μ	610×10^{-9}	MPa s	Apparent fluid viscosity at 170 s^{-1}
Depth	193.5	m	Depth to top of German Creek seam
r	0.048	m	Wellbore radius

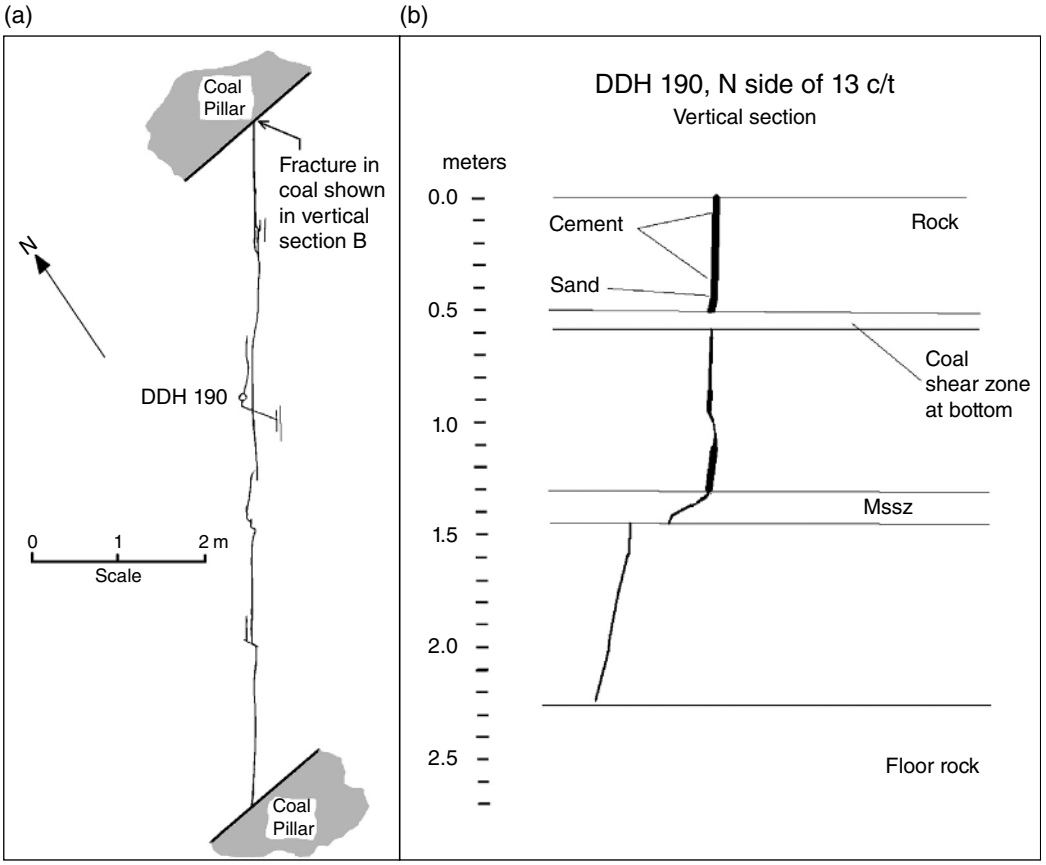

Figure 1.3 Looking down on propped fracture trace (a) in sandstone roof rock at 13 cut-through. Vertical section (b) showing propped fracture exposed on north coal rib of 13 cut-through near borehole DDH 190 (*Source:* Jeffrey et al. [5]/Coalbed Methane Association of Alabama).

ranging from clay size to a few centimeters in size. The mssz is softer and weaker than the coal above and below it. This hydraulic fracture and others mapped in this coal seam often developed an offset across the mssz.

The fracture at DDH 190 extended into the lower stress roof rock with only 12% of the proppant injected estimated to be accounted for by the propped fracture in the coal seam. The mapping clearly shows the trace of the propped hydraulic fracture in the roof and in the coal, but does not reveal if the fracture was growing primarily laterally or vertically at the sections mapped. Modeling of this fracture suggests upward growth of 7 m into the roof rock at the borehole [13].

1.2.2 Fractures in Hard Rock

Hydraulic fracturing is used in mining to induce caving and to precondition rock for caving [7]. More recently, preconditioning has been used in areas of high stress as a means of reducing the potential for the occurrence of large, damaging seismic events [14]. A total of nine fractures have been mined and mapped at four metalliferous mine sites in Australia [7, 9, 15] and Chile [6]. The fractures described by Jeffrey et al. [9] will be compared to the fractures placed into coal seams.

1.2.2.1 Northparkes E48 Mapped Fractures

Six hydraulic fractures were placed ahead of a tunnel at 580 m depth at the E48 Northparkes mine as part of a mine-through experiment [9]. The fractures were propped with colored plastic and sand and were monitored by microseismic and tiltmeter arrays. The mapped hydraulic fractures at Northparkes consist of nearly horizontal segments with offsets at intervals along them produced as the fracture grew into and along dipping veins, natural fractures, and shear zones. Fracture branches and sub-parallel propped sections were also mapped, making up 10–15% of the total fracture extent. The rock mass at the site is naturally fractured, containing approximately five natural fractures per meter. Additional details of the site, fracturing, and mine-back can be found in Jeffrey et al. [9]. Table 1.3 lists site and rock parameters. The stress directions given in Table 1.3 are based on overcoring data measured near the fracture site.

Table 1.3 Site and rock parameters for Northparkes E48.

Parameter	Value	Units	Description
σ_H	40	MPa	Max horizontal stress, 290^0, 8^0 dip
σ_h	22	MPa	Min horizontal stress, 22^0, 11^0 dip
σ_v	15	MPa	Vertical stress, 165^0, 76^0 dip
P_o	<1	MPa	Pore pressure
k	0.005	md	Permeability, millidarcy
E	50 000	MPa	Young's modulus
ν	0.2		Poisson's ratio
Q	0.007 5	m^3/s	Injection rate
μ	610×10^{-9}	MPa s	Apparent crosslinked gel viscosity at $170\ s^{-1}$
	1×10^{-9}	MPa s	Viscosity of water
Depth	580	m	Depth below surface
r	0.048	m	Wellbore radius

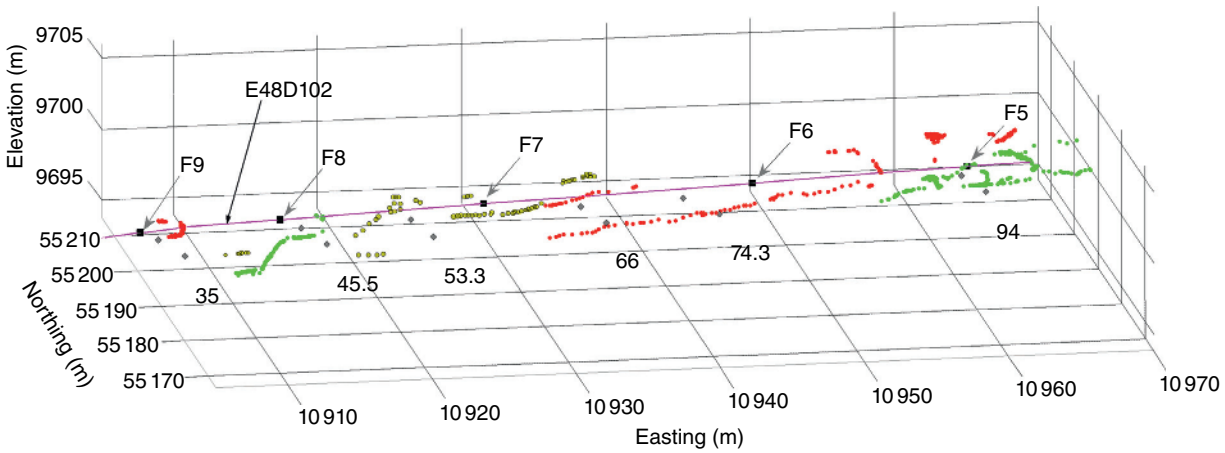

Figure 1.4 Hydraulic fractures mapped along a tunnel at the Northparkes E48 mine (*Source:* Jeffrey et al. [9]/Society of Petroleum Engineers). The initiation point of each fracture is indicated along the borehole which is drawn with a purple line.

The minimum stress was nearly vertical with the maximum stress oriented nearly horizontal and directed approximately east–west.

The hydraulic fractures were mapped along the E48D102 tunnel as it was driven. The fractures were horizontal with steps along their path often forming where they interacted with natural fractures and shear structures. These offsets were large enough to increase the average dip because the fracture trace following a stair-step pattern. Figure 1.4 shows an overview of the five fractures that were propped with colored plastic and mapped along the sides of the tunnel.

Fractures 6 and 7 were placed using crosslinked guar gel while fractures 5, 8, and 9 were placed using water. The colors of the points mapped along each fracture shown in Figure 1.4 correspond to the colors of the plastic proppant used. The grid lines shown are the mine coordinates in meters. The initiation point of each fracture is indicated by a black square symbol and the borehole is shown by the line connecting these symbols. Figure 1.5 contains a more detailed sketch of Fracture 8, which contained the largest offset or step mapped in any of the fractures at this site. The injection interval, which was in the borehole E48D102, is shown. This interval is located approximately 2.5 m out of the plane of the fracture trace shown because the borehole was drilled along the centerline of the tunnel. Fracture growth is likely to have been semi-radial from the injection interval and should not be visualized as occurring purely along the fracture trace. Fracture 7 contained an offset similar in size to the one shown in Figure 1.5 and a series of smaller offsets (but consisting of 200–400 mm steps) were

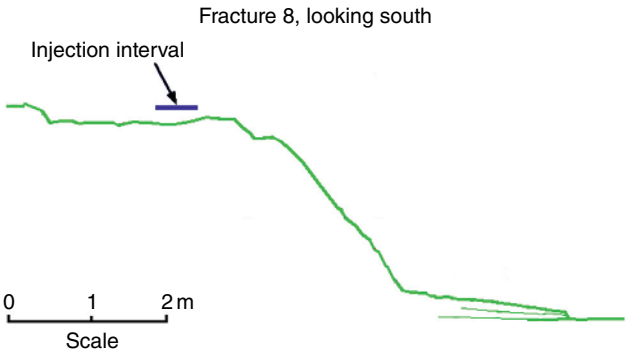

Figure 1.5 The mapped trace of fracture 8, exposed along the south side of the tunnel, at the Northparkes E48 mine-back site (*Source:* Jeffrey et al. [15]).

mapped at one exposure of Fracture 5. Therefore, at this site the crosslinked gel did not produce more planar fractures compared to the water driven fractures.

Details of the fracture geometry were not collected except along the sides of the tunnel and occasionally across the tunnel face and back. This is a common difficulty experienced when mapping hydraulic fractures in a commercial mine. The tunnelling or coal extraction operations take precedence over mapping. In the case of the E48 site, the tunnel is extended in approximately four-meter intervals using a drill-blast-muck-support cycle. Mapping is restricted to occur between the muck and support or support and drill steps.

1.2.3 Other Mapped Fractures

Hydraulic fractures have been placed into a range of rock and soil materials followed by mining and mapping. Warpinski et al. [16] and Warpinski and Teufel [2] describe hydraulic fractures placed into volcanic tuff and Murdoch [1] describe fractures placed into clay and soil at shallow depth. Details of these fractures can be found in the papers cited.

1.3 Comparison of Mapped Fracture Geometries

Nondimensional parameters are useful in helping to determine the type of fracture growth to expect in different rocks and at different sites. For example, the dimensionless toughness or dimensionless viscosity can be used to determine if the treatment was carried out in the fracture toughness or fluid viscosity dominated regime [17]. Viscosity dominated growth leads to more planar fracture geometries [18].

The fracture width restrictions resulting from offsets and branches along the fracture path are potential sites for proppant bridging and the narrow width at these locations result in a higher injection pressure and slower fracture growth compared to more planar fracture conditions [19]. The growth of closely spaced fractures has been shown to be well described by several dimensionless parameters [8, 20]. Results from numerical calculations of the path of a new fracture placed next to an existing fracture were presented by Bunger et al. [20] and were compared to mine-back and laboratory experiments in Bunger et al. [8]. The fractures mapped and described above will be compared with each other and are further categorized by calculating values for the dimensionless viscosity and differential stress parameters.

1.3.1 Dimensionless Parameters

The nondimensional parameters used are listed in Table 1.4. The physical parameters that are used in defining the nondimensional parameters are listed in Table 1.1. The nondimensional viscosity is used to determine whether the fracture growth is dominated by rock fracture toughness or by frictional losses associated with viscous fluid flow in the fracture channel [17]. The dimensionless stress is commonly used in studies of hydraulic fractures interacting with other hydraulic fractures or crossing natural fractures [8, 18, 19]. Two values of dimensionless differential stress are defined because a hydraulic fracture growing with an

Table 1.4 Dimensionless groups used in comparisons.

Name	Parameter	Notes
Dimensionless viscosity	$M = \frac{3\pi^2 \mu Q_0 E'^3}{256 K_{Ic}^4}$	If $M < 0.25$, regime is toughness dominated. If $M > 1$, regime is viscosity dominated.
Dimensionless differential stress	$d_{13} = \frac{(\sigma_1 - \sigma_3)}{\sigma_3}$	d_{13} applies to fracture growth in the direction of σ_1.
Dimensionless differential stress	$d_{23} = \frac{(\sigma_2 - \sigma_3)}{\sigma_3}$	d_{23} applies to fracture growth in the direction of σ_2.

Table 1.5 Nondimensional parameters for three sites.

Site	M	d_{13}	d_{23}
Northparkes F8	7.7	1.7	0.5
DHM-7	4.5	0.4	0.3
DDH 190 coal	3.3	0.8	0.6
DDH 190 roof	2000	1.5	0.7

orientation such that it opens against σ_3 will be subject to a range of differential stresses, depending on the location of the point being considered with respect to the other two principal stresses. These parameters are therefore used here as reference values in the comparisons of overall fracture growth behavior as determined by mine-back mapping.

The values of the three dimensionless parameters at each of the three mapping sites are listed in Table 1.5.

1.4 Fracture Geometry Summary

The M value listed for the Northparkes site applies to fractures created using water, which was the case for Fracture 8, while the treatment in DHM-7 used linear gel and a crosslinked gel was used in DDH 190. The M values below 0.25 represent a fracture regime that is toughness dominated while an M value of one or greater is viscosity dominated. All of the fractures described here fall into the viscosity dominated regime. The fracture growth regime for the part of the fracture that extended into the roof rock at DDH 190 was strongly viscosity dominated.

Natural fractures and shear zones were crossed by the hydraulic fractures at all three sites. The downward growth of the fracture at the DDH 190 site was blunted by a soft clay at the coal-floor rock interface.

Fracture 8 at Northparkes entered a 45° dipping natural fracture and grew along it for approximately 2.5 m before exiting down dip. The exit point coincides with additional calcite mineralization in the natural fracture. This section of the structure would be stronger in shear, resulting in higher shear-generated tensile stress and we propose that this allowed tensile fractures or wing fractures [21] to form at that location, allowing the hydraulic fracture to escape the natural fracture.

Table 1.6 provides a summary of the features that are present in the fractures at the three sites for two different resolutions. The resolution is defined as the smallest feature on the hydraulic fracture that is included in describing the fracture geometry. In Table 1.6, nonplanar means the main fracture channel is not in a single plane while branching means the fracture treatment has propped several fractures over parts of its extent that may be parallel or at an angle to the main fracture.

The propped fracture at the DHM-7 site was T-shaped, with each segment planar when viewed with a resolution of 1 m. When viewed in more detail (with a resolution of 0.01 m) offsets and branches are apparent as shown in Figures 1.1 and 1.2. A T-shaped fracture is considered to be a branched fracture, because the horizontal and vertical segments are both considered as branches of the fracture channel. In Table 1.6, the DHM-7 fracture is considered to be nonplanar and branched at the coarser resolution. T-shaped fractures represent a case where the hydraulic fracture is diverted into the horizontal direction rather than crossing the horizontal feature and continuing to grow vertically. Horizontal fractures associated with T-shaped fractures have been mapped to extend 10–100 s of meters without diverting back into the coal or up into the roof. The mechanics of this observed feature of these fractures has not been completely explained.

The qualitative description in Table 1.6 shows that the classification regarding planarity, branches, and offsets depends on the scale of the observation. When a more detailed view is available, the fractures at all the sites show offset, nonplanar, and branched growth. The main factor that controls the development of these features in a hydraulic Efracture is the presence of natural fractures or bedding interfaces. The fracture growth regime and the deviatoric stress, at least in the range represented by the three sites reviewed here, do not seem to result in a strong change

Table 1.6 Fracture geometry versus resolution of observation.

	Resolution 1 m			Resolution 0.01 m		
Site	Offsets	Nonplanar	Branching	Offsets	Nonplanar	Branching
Northparkes	Yes	Yes	No	Yes	Yes	Yes
DHM-7	No	Yes	Yes	Yes	Yes	Yes
DDH 190 coal	No	No	No	Yes	Yes	Yes
DDH 190 roof	No	No	No	Yes	Yes	Yes

in the fracture geometry, at least as expressed by mapping of its propped extent. Network like fracture development would be expected as the deviatoric stress is reduced toward zero, but we do not have mapped fractures representing that stress condition.

1.5 Conclusions

Three sites at which hydraulic fractures have been mined and mapped are described. Measured parameters are given for each site that are then used to find the dimensionless viscosity and dimensionless deviatoric stress values for the sites.

The mapped fractures at all three sites are found to be similar in the sense that, when they are studied at a detailed scale, they all contained offsets, were nonplanar, and contained branches. The common factor between all sites is that the rock (or coal) was naturally fractured. The nondimensional parameters were not found to be useful in predicting the amount of offsetting, nonplanar growth, or branching. Mapping fractures at sites with lower deviatoric stress may show a sensitivity to that parameter in predicting network such as fracture development.

References

1 Murdoch, L.C. (1995). Forms of hydraulic fractures created during a field test in Overconsolidated glacial drift. *Quarterly Journal of Engineering Geology* 28: 23–35.

2 Warpinski, N.R. and Teufel, L.W. (1987). Influence of geologic discontinuities on hydraulic fracture propagation. *Journal of Petroleum Technology* 39 (2): 209–220.

3 Diamond, W.P. and Oyler, D.C. (1987). Effects of Stimulation Treatments on Coalbeds and Surrounding Strata. *USBM Report RI 9083*.

4 Elder, C.H. (1977). Effects of Hydraulic Stimulation on Coalbeds and Associated Strata. *USBM Report RI 8260*.

5 Jeffrey, R.G., Enever, J.R., Ferguson, T. et al. (1992). Small-scale hydraulic fracturing and mineback experiments in coal seams. *Proceedings of the 1992 International Coalbed Methane Symposium*, Tuscaloosa, (17–21 May). Paper 9330.

6 Chacon, E.; Barrera, V.; Jeffrey, R.; van As, A. Hydraulic fracturing used to precondition ore and reduce fragment size for block caving. In *MassMin* 2004; Santiago; pp 429–534.

7 van As, A. and Jeffrey, R.G. (2002). Hydraulic fracture growth in naturally fractured rock: mine through mapping and analysis. *5th North American Rock Mechanics Symposium and the 17th Tunnelling Association of Canada Conference*, 9. Toronto: ARMA.

8 Bunger, A.P., Jeffrey, R.G., Kear, J. et al. (2011). Experimental investigation of the interaction among closely spaced hydraulic fractures. *45th US Rock Mechanics/Geomechanics Symposium*. American Rock Mechanics Association. https://www.onepetro.org/conference-paper/ARMA-11-318. Accessed 28 January 2016.

9 Jeffrey, R.G., Bunger, A.P., Lecampion, B. et al. (2009). Measuring hydraulic fracture growth in naturally fractured rock. *Proceedings SPE Annual Meeting*, 18. New Orleans: SPE.

10 Boyer, C.M., Stubbs, P.B., Schwerer, F.C. et al. (1986). Measurement of coalbed properties for hydraulic fracture design and methane production. *Proceedings of the 1986 Unconventional Gas Technology Symposium*, Louisville, (18–21 May). Paper SPE 15258.

11 Steidl, P.F. (1991). Observations of Induced Fractures Intercepted by Mining in the Warrior Basin, Alabama. *GRI Topical Report No. GRI-91/0327*.

12 Boyer, C.M., Stubbs, P.B., Schwerer, F.C., et al. (1986b). Mapping of the DHM-7 Hydraulic Fracture. Appendix I in: Measurement of static coalbed reservoir conditions for hydraulic fracture design; final report, volume II, GRI-**87**/0082.2. Chicago, IL, Gas Research Institute, Dec. 1986.

13 Jeffrey, R.G., Settari, A., and Smith, N.P. (1995). A comparison of hydraulic fracture field experiments, including mineback geometry data, with numerical fracture model simulations. *Proceedings SPE Annual Meeting*, (591–606). Dallas: SPE.

14 Board, Mark, Tony Rorke, Gary Williams, and Nick Gay. "Fluid injection for rockburst control in deep mining." In *The 33rd US Symposium on Rock Mechanics (USRMS)*. 1992.

15 Jeffrey, R.G., Zhang, X. and Bunger, A.P. (2010). Hydraulic fracturing of naturally fractured reservoirs. *Thirty-Fifth Workshop on Geothermal Reservoir Engineering*, 9. Stanford: Stanford University.

16 Warpinski, N.R., Schmidt, R.A., and Northrop, D.A. (1982). In-situ stresses: the predominant influence on hydraulic fracture containment. *Journal of Petroleum Technology* 34 (3 (March)): 653–664.

17 Detournay, E. (2004). Propagation regimes of fluid-driven fractures in impermeable rocks. *International Journal of Geomechanics* 4 (1): 35–45.

18 Weng, X., Kresse, O., Chuprakov, D. et al. (2014). Applying complex fracture model and integrated workflow in

unconventional reservoirs. *Journal of Petroleum Science and Engineering* 124: 468–483. https://doi.org/10.1016/j.petrol.2014.09.021.

19 Zhang, X. and Jeffrey, R.G. (2006). The role of friction and secondary flaws on deflection and re-initiation of hydraulic fractures at orthogonal pre-existing fractures. *Geophysical Journal International* 166: 1454–1465.

20 Bunger, A.P., Zhang, X., and Jeffrey, R.G. (2012). Parameters affecting the interaction among closely spaced hydraulic fractures. *SPE Journal-Richardson* 17 (1): 292–306.

21 Fairhurst, C. and Cook, N.G.W. (1966). The phenomenon of rock splitting parallel to the direction of maximum compression in the neighborhood of a surface. *Proceedings First Congress International Society for Rocks Mechanics*. Lisbon.